DOI 10.2478/ama-2019-0021

NON-LINEAR ANALYSIS OF AIR PRESSURE FLUCTUATIONS DURING BUBBLE DEPARTURE SYNCHRONISATION

Paweł DZIENIS*, Romuald MOSDORF*, Tomasz WYSZKOWSKI, Gabriela RAFAŁKO*

*Faculty of Mechanical Engineering, Bialystok University of Technology, Wiejska 45C, 15-351 Białystok, Poland

p.dzienis@pb.edu.pl, r.mosdorf@pb.edu.pl, wyszkowski.tomasz@gmail.com, girejkogabriela@gmail.com

received 27 May 2019, revised 6 September 2019, accepted 10 September 2019

Abstract: In the recent paper, non-linear methods of data analysis were used to study bubble departure synchronisation. In the experiment, bubbles were generated in engine oils from two neighbouring brass nozzles (with an inner diameter of 1 mm). During the experiment, the time series of air pressure oscillations in the air supply system and voltage changes on phototransistor were recorded. The analysis of bubble departure synchronisation was performed using a correlation coefficient. The following methods of non-linear data analysis are considered. Fast Fourier Transformation, autocorrelation, attractor reconstruction, correlation dimension, largest Lyapunov exponent and recurrence plot analysis were used to examine the correlation between bubbles behaviour and character of pressure fluctuations. Non-linear analysis of bubble departure synchronisation revealed that the way of bubble departures from two neighbouring nozzles does not depend simply on the character of pressure fluctuations in the nozzle air supply systems. The chaotic changes of the air pressure oscillations do not always determine the chaotic bubble departures.

Key words: Bubble Departures, Alternative Bubble Departures, Nonlinear Methods of Data Analysis

1. INTRODUCTION

The bubbles–bubbles and bubbles–liquid interactions occur in many technological applications such as hydrocarbon industries, chemical processes, bubble column reactors or boiling heat transfer. Understanding the interactions between moving gas bubbles in oils would be useful in optimising the devices for degassing or transporting oils (Lavensona et al., 2016).

The interactions between bubbles generated in water and silicone oils from two adjacent orifices were discussed in the articles by Sanada et al. (2009), Legendere et al. (2003) and Snabre and Magnifotcham (1997). It was concluded that interactions between bubbles can cause two kinds of bubble behaviours – bubble coalescence and bubble bouncing. The kinds of bubble behaviours depend on Reynold, Morton and Webber numbers concerning bubbles. In the case when bubbles do not coalesce, then the alternative, chaotic or simultaneous bubble departures from neighbouring nozzles occur. The bubbles generated in the water and an aqueous glycerine solution from two neighbouring microtubes were analysed and described in the article by Kazakis et al. (2008). It was shown that bubbles–bubbles interactions depend on liquid properties, gas flow rate and distance between the tubes. Alternative bubble departures were investigated by Mosdorf and Wyszkowski (2011, 2013). The mentioned works confirm that bubbles departed from neighbouring nozzles interact with each other. Interactions between bubbles cause the moving bubbles to form unique structures above nozzle outlets. During alternative bubble departures, bubbles depart periodically. Such interactions modify the hydrodynamic condition above the nozzle outlets. Consequently, they modify the air pressure oscillations in air supply systems (Fermat et al., 1998; Vazques et al., 2010; Dzienis and Mosdorf, 2014). The synchronisation of bubble departures from neighbouring nozzles related to air pressure changes is not fully understood.

Vezques et al. (2010), Dzienis and Mosdorf (2014) and Mosdorf et al. (2017) suggested that bubbles behaviour over the nozzle's outlet is correlated with air pressure fluctuations. Usually, both bubbles behaviour and pressure fluctuations have a chaotic character. In the recent article, pressure signals recorded in two nozzles (with an inner diameter of 1 mm) of the gas supply system are investigated using methods of non-linear data analysis. The following methods of non-linear data analysis were used: Fast Fourier Transformation, autocorrelation, attractor reconstruction, correlation dimension, largest Lyapunov exponent and recurrence plot (RP) analysis. The analysis was conducted for an almost periodic bubble departure processes. The process was almost periodic but not completely correlated with the air pressure changes in the air supply system. The changes in time of alternative and simultaneous bubble departures were observed. In this article, the correlation between bubbles behaviour and pressure fluctuations character is examined. The recent article shows that the character of bubble departures from two neighbouring nozzles does not depend simply on the pressure fluctuations in the nozzle air supply systems. The chaotic changes in the air pressure oscillations do not always determine the chaotic bubble departures.

2. EXPERIMENTAL SETUP AND DATA CHARACTERISTICS

In the experiment, bubbles were generated from two neighbouring brass nozzles to the glass tank with the dimensions

of 400×400×700 mm. The tank (Fig. 1 – 2) was filled with mineral engine oil. Nozzles with an inner diameter of 1.1 mm (Fig. 1 – 1) were placed at the bottom of a tank. The distance (*S*) between nozzles was equal to 4 mm. The scheme of the experimental setup is shown in Fig. 1.

The air was supplied to air tanks using air pumps (Fig. 1 – 9). The air pressure was set using the proportional pressure reducing valves – Metalwork Regtronic (Fig. 1 – 7). The adjustable pressure range of pressure reducing valve was 0.05–10 bar. The accuracy of the pressure reducing valve was 0.5%. During the experiment, the air pressure was equal to 0.2 bar. The air volume flow rate was measured using flow meters – MEDSON s.c Sho-Rate-Europe Rev D, P10412A (Fig. 1 – 4) with an accuracy of 5%. The air volume flow rate was in the range of 0.014 L/min to 0.125 L/min. During the experiment, the temperature of the liquid was approximately 20°C. The temperature of the liquid was controlled by the digital thermometer – MAXIM DS18B20.

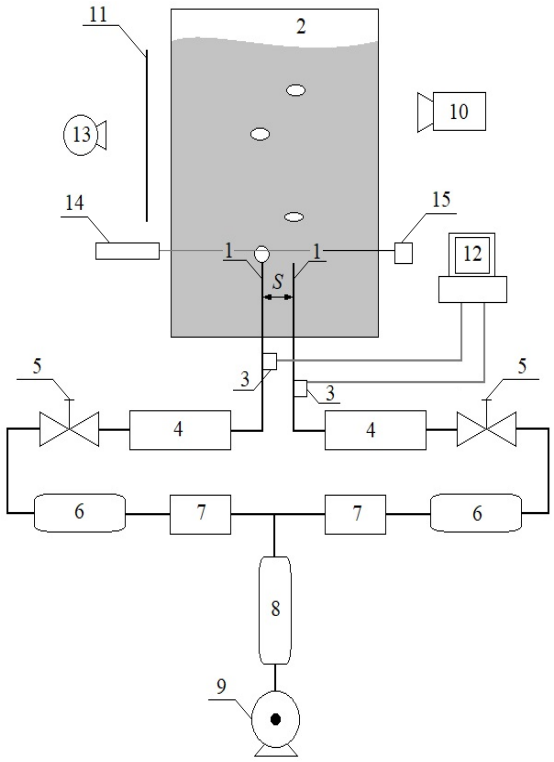

Fig. 1. Schema of experimental setup. 1 – nozzles, 2 –glass tank, 3 – pressure sensors, 4 – flow meters, 5 – air valves, 6 – air tanks, 7 – pressure regulators, 8 – air tank, 9 – air pomp, 10 – high speed camera, 11 – shutter, 12 – data acquisition station, 13 – light source, 14 – laser, 15 – phototransistor

In the experiment, bubble movement, time series of voltage changes on phototransistor and pressure changes in the gas supply system were recorded. Bubble movement was recorded using a high-speed camera – CASIO EX FX 1 (Fig. 1 – 10). Videos were recorded in grey scale with a speed of 600 fps. The gathered films were divided into frames. The example video frames are shown in Fig. 2.

In Fig. 2, two subsequent frames of bubble chain formation are presented for air volume flow rates of 0.0260 L/min and 0.0657 L/min. The time period between frames marked with I and II in Fig. 2 is equal to 0.039 s. When the air volume flow rate is q = 0.0260 L/min, then two bubbles coalesce above nozzle outlets (Fig. 2). When the air volume flow rate is 0.0657 L/min, then four bubbles coalesce above the nozzle outlet. The different number of coalesced bubbles causes a decrease in the distance between subsequent bubbles. Despite the fact that the frequency of bubble departures is the highest in the case presented in Fig. 2b, the bubble distance is greater in comparison with the mentioned distance in Fig. 2a.

Air pressure fluctuations were measured with the silicon pressure sensor – Frescale Semiconductor MPX12DP (Fig. 1 – 3). Time series of pressure changes were recorded using data acquisition station DT9800 (Fig. 1 – 12) with a sampling frequency of 1 kHz. The time series for particular air volume flow rates (*q*) are presented in Fig. 3.

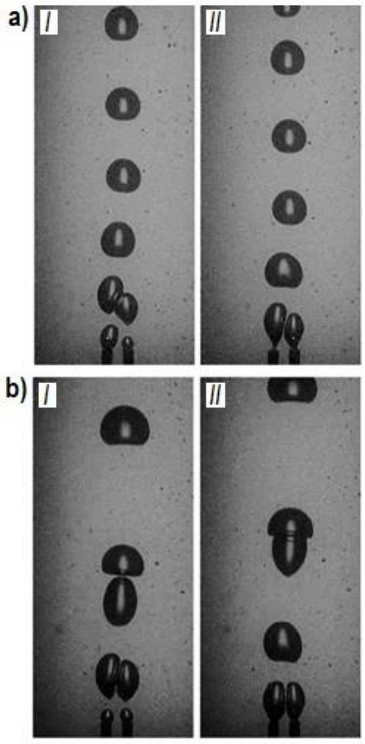

Fig. 2. The example frames of recorded videos. (a) Air volume flow rate *q* = 0.0260 L/min (alternative bubble departures happen – frame *I*) and (b) air volume flow rate *q* = 0.0657 L/min (simultaneous bubble departures happen – frame *II*)

Pressure oscillations in gas supply systems for air volume flow rate *q* = 0.0260 L/min are presented in Fig. 3a (left nozzle) and Fig. 3b (right nozzle). In the time series of pressure changes in both nozzles, the following phenomena appear: pressure fluctuations caused by bubble departures and long-term pressure oscillations. The long-term pressure oscillations decrease in the left nozzle as the expenditure increases the air volume flow rate (Fig. 3). In this case, the bubbles departed in an almost periodic way. In the right nozzle, long-term pressure oscillations occurred despite the increase of air volume flow rate (Fig. 3d). In this case, the bubbles departed in a non-periodic way. The occurrence of long-term pressure oscillations and the different characters of bubble departures lead the authors of this article to use non-linear methods of data analysis to study the interactions between departed and growing bubbles.

Moreover, during the experiment, the bubble growing time was measured using a laser–phototransistor system. The laser beam was placed approximately 1 mm above the nozzle outlets. The process of bubble growing caused the interruption of the laser

DOI 10.2478/ama-2019-0021

beam. The voltage on the phototransistor for the bubble growth was equal to ~0.2 V. After the bubble departure, the laser beam was not interrupted. At this moment, the value of the voltage was equal to ~4.8 V. Time series of voltage changes on phototransistor were recorded simultaneously with a time series of pressure fluctuations.

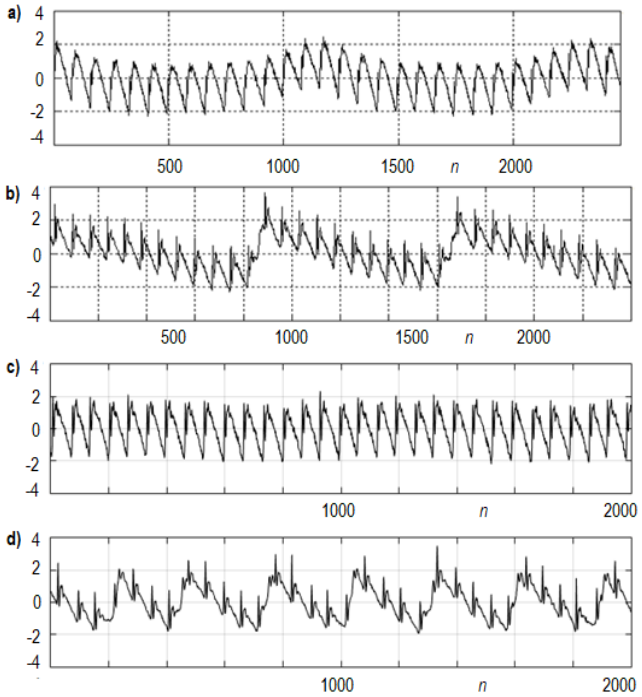

Fig. 3. The time series of pressure changes in gas supply system in the left and right nozzles: (a) q = 0.0260 L/min, left nozzle; (b) q = 0.0260 L/min, right nozzle; (c) q = 0.0657 L/min, left nozzle and (d) q = 0.0657 L/min, right nozzle

In order to determine the duration of the simultaneous and alternative bubble departures, the correlation coefficient (Cor) was calculated in the moving window of time which is equal to a single cycle of bubble departures (~0.14 s for 85 samples, Fig. 3a and b; ~0.12 s for 71 samples, Fig. 3c and d). *Cor* was calculated according to the following formula:

$$Cor = \frac{Cov(x_{i,L},x_{i,R})}{\sigma_{x,L},\sigma_{x,R}} \quad (1)$$

where: *cov* is the covariance, σ is the standard deviation of signal, $x_{i,L}$ denotes the time series of pressure fluctuations in left nozzle and $x_{i,R}$ is the time series of pressure fluctuations in the right nozzle.

When *Cor* tends to 1 or −1, then time series $x_{i,L}$ and $x_{i,R}$ are correlated. When *Cor* is close to 0, then the time series $x_{i,L}$ and $x_{i,R}$ are not correlated. When value *Cor* is close to 1, then bubbles depart (from twin nozzle) at the same time. When the value of *Cor* is negative, then bubbles depart alternatively. The changes of *Cor* for pressure fluctuations time series are presented in Fig. 4.

The correlation coefficient was calculated for a time series of pressure fluctuations (dotted lines – Fig. 4) and time series from phototransistor (solid line – Fig. 4). The correlation coefficient evaluated from phototransistor signals is helpful to determine the time period of alternative or simultaneous bubble departures.

In the case presented in Fig. 3a (q = 0.0260 L/min), alternative bubble departures occur during five subsequent cycles of bubble departures and are interrupted by two acts of simultaneous bubble departures. In Fig. 3b, the occurrence period of alternative bubble departures is equal to 10 cycles. The reappearance of alternative bubble departures takes place after three cycles of simultaneous bubble departures. It can be concluded that the increase of air volume flow rate causes an elongation of the alternative bubble departure occurrence period.

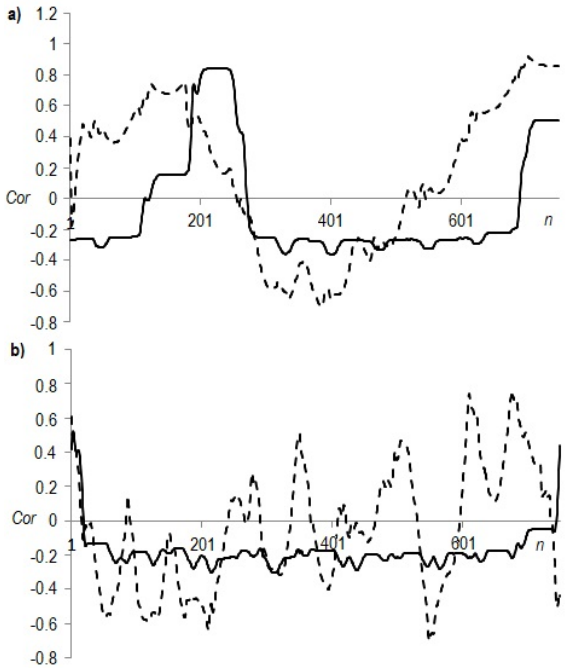

Fig. 4. The correlation coefficient, *Cor*, changes for pressure fluctuations (dotted lines) and phototransistor signals (solid lines): (a) q = 0.0260 L/min and (b) q = 0.0657 L/min

During the alternative bubble departures (presented in Fig. 3b), intense, chaotic fluctuations of the air pressure correlation coefficient were observed. During the alternative bubble departures (presented in Fig. 3a), the value of the correlation coefficient increased continuously and its oscillations were weaker in comparison with the case presented in Fig. 3b.

3. NON-LINEAR ANALYSIS OF PRESSURE FLUCTUATIONS

The following methods of non-linear data analysis are used in this study:

- the frequency analysis – Fast Fourier Transformation,
- autocorrelation,
- attractor reconstruction,
- calculation of correlation dimension and largest Lyapunov exponent, and
- RP analysis.

3.1 The frequency analysis

The frequency of bubble departures is constant during periodic bubble departures; but when bubbles depart chaotically, then the frequency of bubble departures is variable. The observation proves that analysis of bubble departures' frequency

is complicated. Therefore, to estimate the frequency of bubble departures, the Fourier Transformation was introduced. The Fourier Transformation evaluates the time-domain data in the frequency domain, which is treated as bubble departures' frequency. The Fourier Transformation has the following form (Torrence and Compo, 1998):

$$F_k = \sum_{n=0}^{n-1} x_n e^{-j\frac{2\pi}{n}kl} \tag{2}$$

The power spectrum is defined as $P=|F_k|^2$. Power spectrums for time series of pressure changes in gas supply systems are shown in Fig. 5.

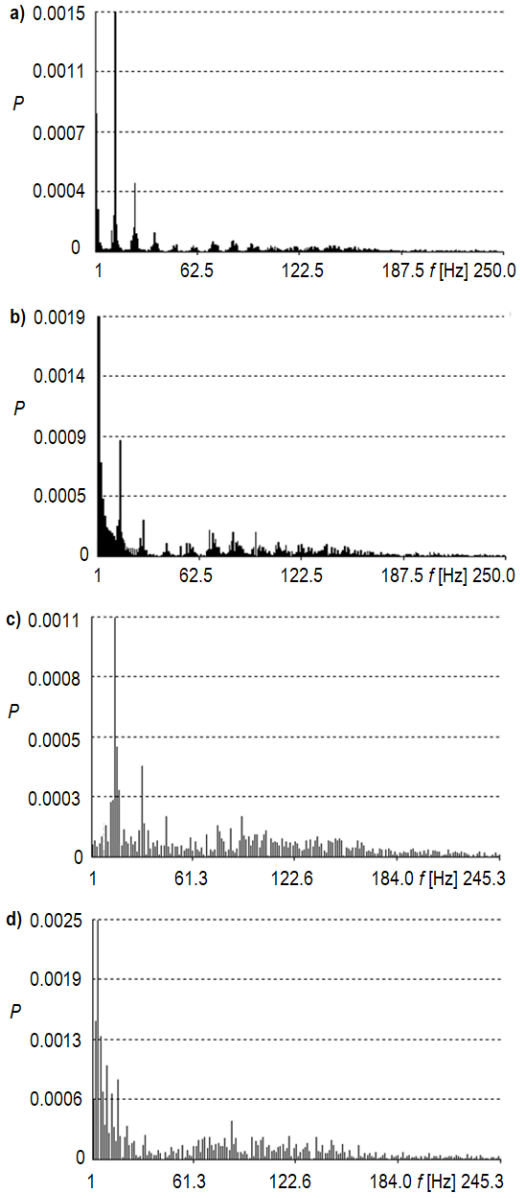

Fig. 5. Fourier power spectrums for time series of pressure changes in gas supply systems for left and right nozzles: (a) q = 0.0260 L/min, left nozzle; (b) q = 0.0260 L/min, right nozzle; (c) q = 0.0657 L/min, left nozzle and (d) q = 0.0657 L/min, right nozzle

In Fig. 5, the power spectrums for pressure changes in the right and left nozzles were calculated separately. In Fig. 5a and c, the dominant frequency of pressure fluctuations indicates the bubble departure frequency (13.59 Hz – Fig. 5a; 16.14 Hz – Fig. 5c). Fig 5b and d illustrates that the dominant frequency of pressure fluctuations are connected with the long-term pressure fluctuations (connected with the disappearance of alternative bubble departures). The frequencies of the bubble departures are evaluated using the 'second dominant frequency' (12.62 Hz – Fig. 5b; 15.95 Hz – Fig. 5d).

An increase in air volume flow rate diminishes the differences between frequencies of bubble departures from the left and right nozzle in comparison with the case presented in Fig. 5a and b.

3.2 Attractor reconstructions

The attractor reconstruction was carried out using the stroboscope coordination (Schuster, 1993). This method calculates subsequent coordinates of attractor points based on the samples between which the distance is equal to time delay. The time delay influences the attractor shape. In the recent article, the time delay was estimated using a method based on the analysis of autocorrelation function (Ca). The time delay (τ) was calculated using the following criterion (Grassberger and Procaccia, 1983):

$$C_a(\tau) \sim 0.5 C_a(0) \tag{3}$$

where C_a is defined as (Schuster, 1993):

$$C_a(\tau) = \frac{1}{N}\sum_{i=0}^{n} x_i x_{i+\tau} \tag{4}$$

where: N is the number of samples and x_i is the value of i sample.

The function (4) is constant or oscillates when τ increases for data generated by the periodical system (Schuster, 1993). In the case of chaotic data, the value of the autocorrelation function rapidly decreases when τ increases.

The attractor reconstruction was carried out using the stroboscope coordination (Schuster, 1993). This method calculates subsequent coordinates of attractor points based on the samples between which the distance is equal to time delay. The time delay influences the attractor shape. In the recent article, the time delay was estimated using a method based on the analysis of autocorrelation function (C_a). The time delay (τ) was calculated using the following criterion (Grassberger and Procaccia, 1983):

$$C_a(\tau) \sim 0.5 C_a(0) \tag{3}$$

where C_a is defined as (Schuster, 1993):

$$C_a(\tau) = \frac{1}{N}\sum_{i=0}^{n} x_i x_{i+\tau} \tag{4}$$

where N is the number of samples and x_i is the value of i sample.

The function (4) is constant or oscillates when τ increases for data generated by the periodical system (Schuster, 1993). In the case of chaotic data, the value of the autocorrelation function rapidly decreases when τ increases.

In Fig. 6, the autocorrelation functions for time series of pressure fluctuation in gas supply systems for the left and right nozzles are presented.

Considering the air volume flow rate q = 0.0260 L/min (Fig. 6a and b), the time delay (τ) is equal to 17 and 41 for the left nozzle and right nozzle, respectively. When the air volume flow rate is equal to q = 0.0657 L/min, the time delay (τ) is equal to 11 for the left nozzle and 28 for the right nozzle.

DOI 10.2478/ama-2019-0021

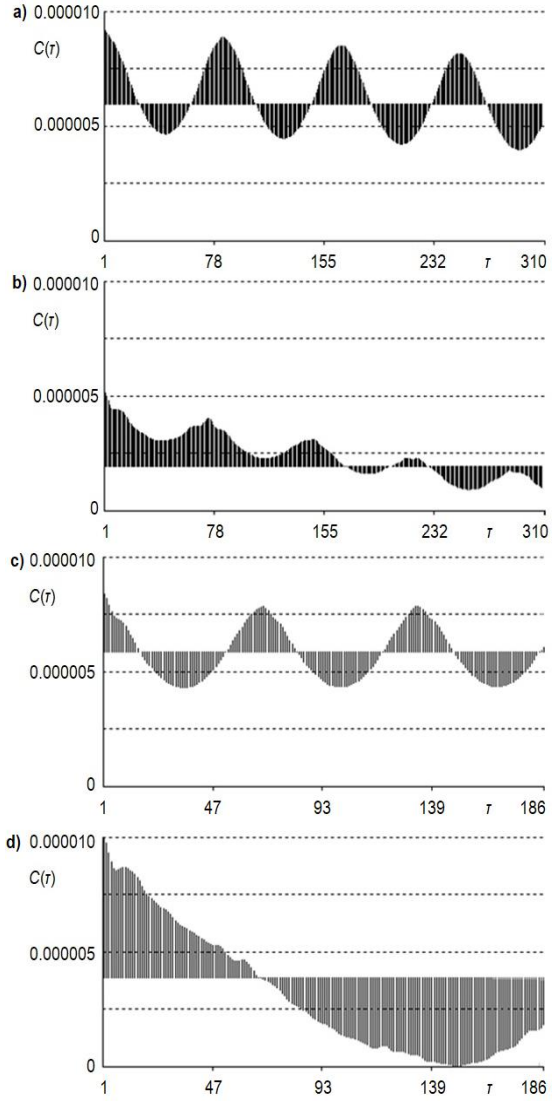

Fig. 6. Autocorrelation functions for time series of pressure fluctuation in gas supply system for the left and right nozzles: (a) q = 0.0260 L/min, left nozzle; (b) q = 0.0260 L/min, right nozzle; (c) q = 0.0657 L/min, left nozzle and (d) q = 0.0657 L/min, right nozzle

The values of time delay were used to form the reconstructions of three-dimensional (3D) attractors. The 3D attractor reconstructions for time series of pressure changes are presented in Fig. 7.

For the air volume flow rates q = 0.0260 L/min – left nozzle (Fig. 7a) and q = 0.0657 L/min – left nozzle (Fig. 7c), the reconstructed trajectories of 3D attractors form a torus. It indicates that the bubble departures are quasiperiodic. The shapes of trajectories presented in Fig. 7b and d do not form a torus. According to this observation, a chaotic character of bubble departures is assumed.

The correlation dimension, D_2, is one of the characteristics of the attractor. In the recent article, the correlation dimension was calculated using Grassberger–Procaccia algorithm (Grassberger and Procaccia, 1983), where:

$$D_2 = \lim_{r\to 0} \frac{1}{\ln r} \ln \sum_i p_i^2 \tag{5}$$

$$\sum_i p_i^2 \approx \lim_{N\to\infty} \frac{1}{N^2} \sum_{i,j} \Theta\left(r - \left|\overrightarrow{x_i} - \overrightarrow{x_j}\right|\right) \tag{6}$$

where: $\Theta(x)$ is Heaviside's step function, p is the probability, r is distance, x_i is the time series of pressure fluctuations in the left nozzle and x_j is the time series of pressure fluctuations in the right nozzle.

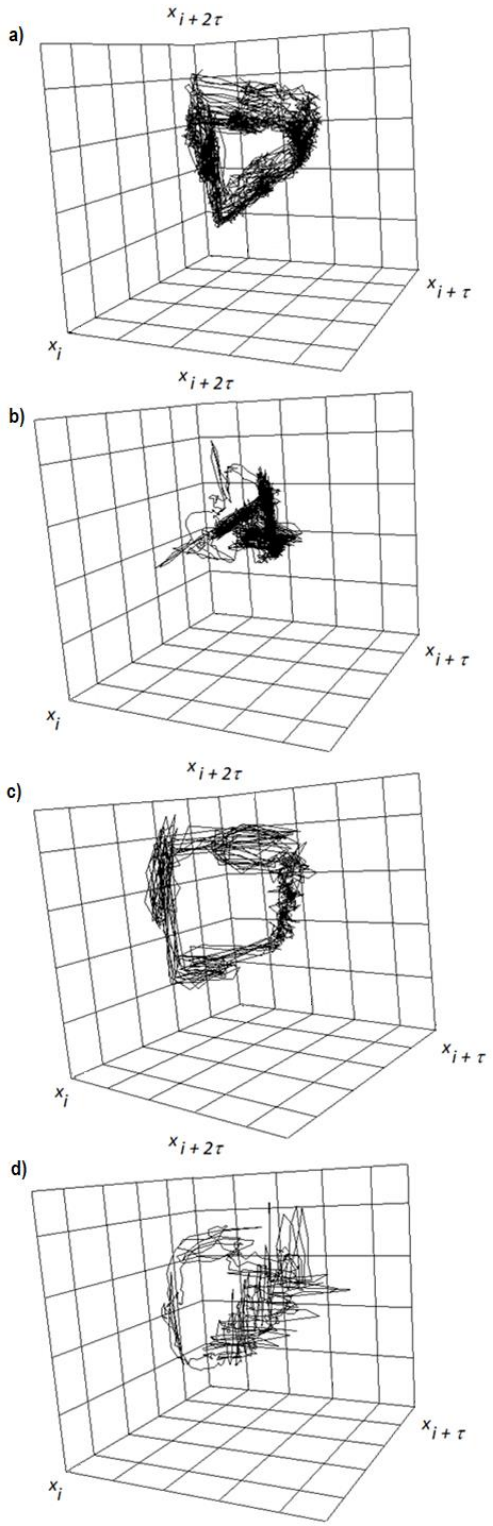

Fig. 7. The three-dimensional attractor reconstructions for time series of pressure changes in gas supply system for left and right nozzles: (a) q = 0.0260 L/min, left nozzle; (b) q = 0.0260 L/min, right nozzle; (c) q = 0.0657 L/min, left nozzle and (d) q = 0.0657 L/min, right nozzle

The graphs of log(*C*) function of log(*r*) for the analysed time series were shown in Fig. 8.

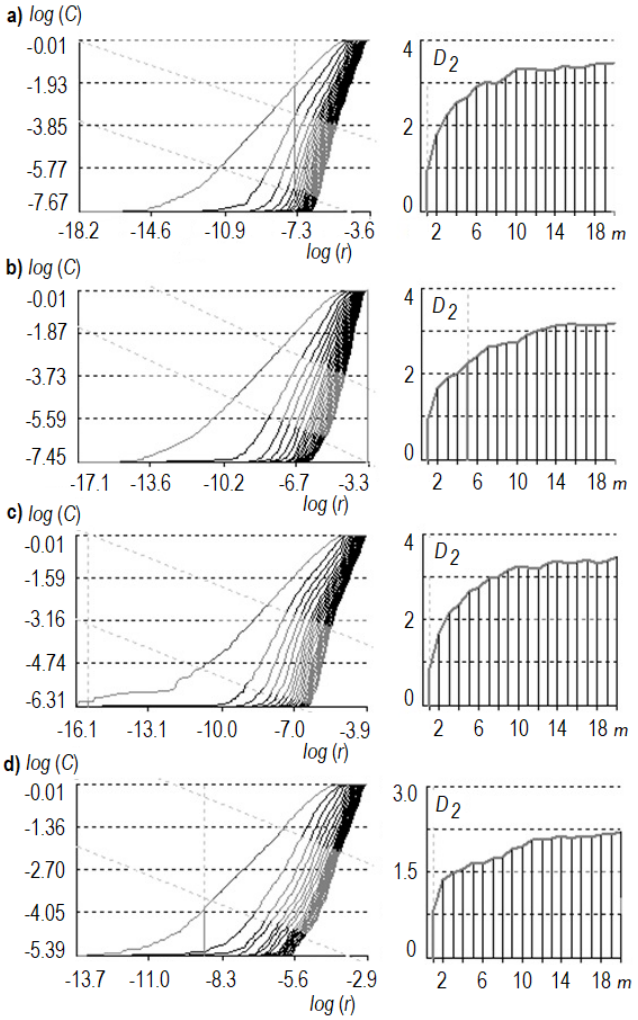

Fig. 8. Graphs of log(C) versus log(r) and correlation dimensions for time series of pressure changes in gas supply systems for left and right nozzles: (a) q = 0.0260 L/min, left nozzle; (b) q = 0.0260 L/min, right nozzle; (c) q = 0.0657 L/min, left nozzle and (d) q = 0.0657 L/min, right nozzle

The correlation dimension D_2 is equal to 4 for both analysed nozzles when the air volume flow rate is q = 0.0260 L/min (Fig. 8a and b). For the air volume flow rate q = 0.0657 L/min, D_2 is 4 (Fig. 8c) and 3 (Fig. 8d) for the left nozzle and right nozzle, respectively.

3.3 Largest Lyapunov exponent

The largest Lyapunov exponent is helpful to identify the intensity of chaotic changes of analysed time series. The largest Lyapunov exponent is calculated according to the following formula (Wolf et al., 1985):

$$\lambda = \sum_{j=1}^{m} \log_2 \frac{d(x_{j+1})}{d(x_j)} \tag{7}$$

In the process of Largest Lyapunov exponent estimation, two points of the attractor (reconstructed for time series) immersed in m-dimensional space are selected. The distance between these points is marked as $d(x_j)$ and is calculated after one orbiting period. After a certain time, the distance between the selected points is calculated again. This distance is denoted as $d(x_{j+1})$.
The values of the largest Lyapunov exponent for analysed time series are shown in Fig. 9.

The value of λ is evaluated as the last value of the curve in the graph (Fig. 9). When the air volume flow rate q = 0.0260 L/min, then the largest Lyapunov value calculated is 31.35 (Fig. 9a) and 58.84 (Fig. 9b) for the left and right nozzles, respectively. For the value of air volume flow rate q = 0.0657 L/min, the largest Lyapunov exponent equals to 39.20 and 90.07 for the left and right nozzles, respectively (Fig. 9c and d).

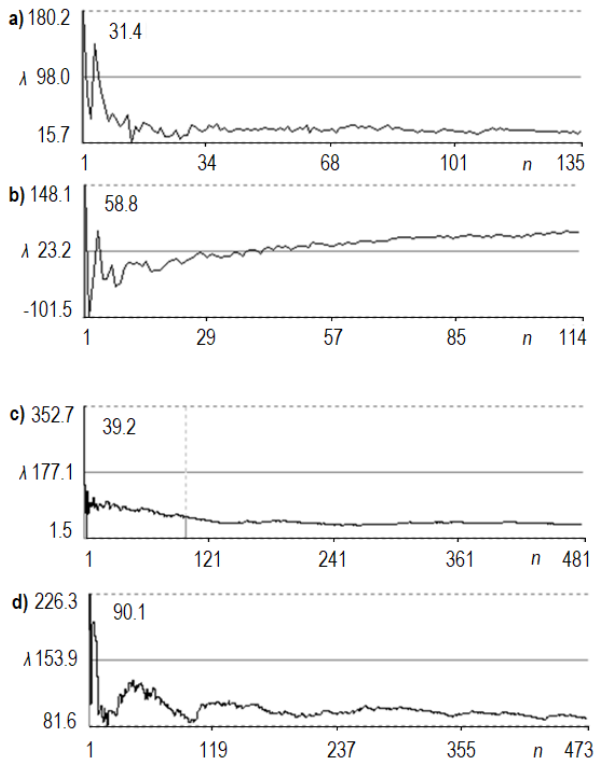

Fig. 9. The largest Lyapunov exponent for time series of pressure changes in gas supply systems for left and right nozzles: (a) q = 0.0260 L/min, left nozzle; (b) q = 0.0260 L/min, right nozzle; (c) q = 0.0657 L/min, left nozzle and (d) q = 0.0657 L/min, right nozzle

3.4 RP analysis

In order to determine the repeatability of the pressure changes in the gas supply system in the subsequent cycles of bubble departures, RPs were used. RP is the technique of visualisation of the recurrence of states in m-dimensional phase space. The recurrence of a state at the time i at a different time j is marked with black dots in the plot. In the RP, vertical and horizontal axes represent time. The RP is defined as (Marwan et al., 2007):

$$R_{i,j} = \Theta\left(\varepsilon_i - \left\|x_i - x_j\right\|\right), \quad x_i \in \Re^n, \quad i,j = 1 \ldots N \tag{8}$$

where N is the number of considered states x_i, ε is the threshold distance for states which are identified as the same, $\|\cdot\|$ is a norm and $\Theta(\cdot)$ is the Heaviside function.

DOI 10.2478/ama-2019-0021

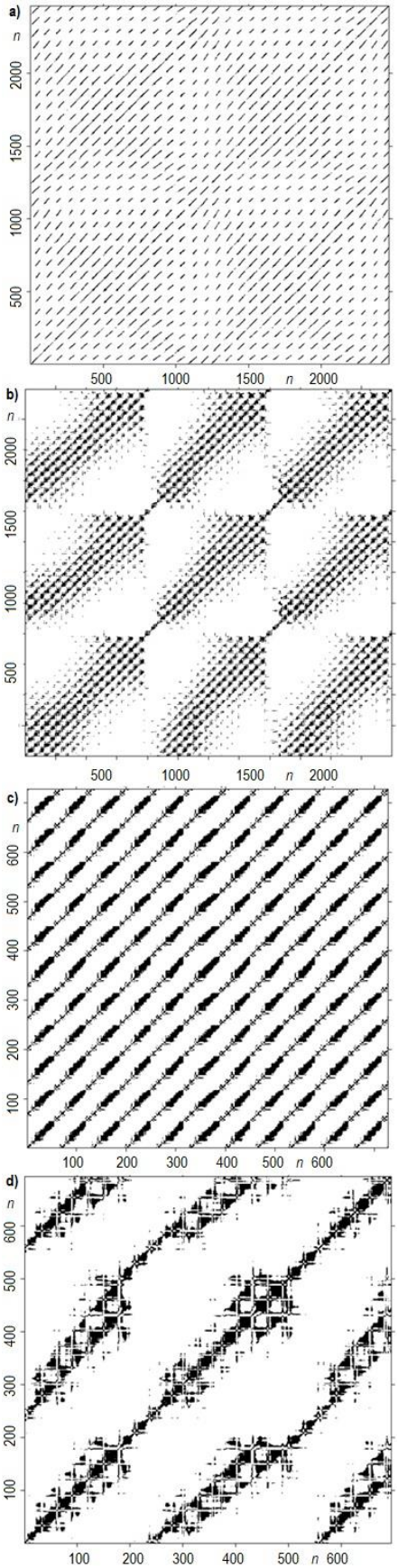

Fig. 10. The recurrence plots for time series of pressure changes in gas supply systems for left and right nozzles: (a) q = 0.0260 L/min, left nozzle; (b) q = 0.0260 L/min, right nozzle; (c) q = 0.0657 L/min, left nozzle and (d) q = 0.0657 L/min, right nozzle

In Fig. 10, the RPs for analysed time series are presented. RPs were calculated using the CRP toolbox implemented by Marwan (2019) in Matlab. Periodic oscillations of pressure create the parallel diagonal lines on RP. The distance between diagonal lines indicates the time between subsequent bubble departures. The RP shown in Fig. 10a and c proves that bubbles from the left nozzle departed almost periodically. The gaps between diagonal lines are created by small chaotic pressure fluctuations occurred after the bubble departures. The RP presented in Fig. 10b and d indicates that pressure fluctuations have a chaotic character (in the right nozzles).

Quantity analysis of RP presented in Fig. 10 was calculated using the following coefficients:

- Recurrence rate (*RR*) determines the percentage of recurrence points in the RP:

$$RR = \frac{1}{N^2} sum_{i,j=1}^{N} R_{i,j}$$

- Averaged diagonal line length:

$$L = \frac{\sum_{l=l_{min}}^{N} lP(l)}{\sum_{l=1}^{N} P(l)}$$

- Trapping time is the average length of the vertical lines:

$$TT = \frac{\sum_{v=v_{min}}^{N} vP(v)}{\sum_{v=v_{min}}^{N} vP(v)}$$

where N is the number of points on the phase space trajectory, $P(l)$ and $P(v)$ denote histogram of the line lengths of diagonal and vertical lines, respectively.

The obtained values of coefficients are presented in Table 1.

Tab. 1. The values of recurrence rate (*RR*), averaged diagonal line length (*L*) and trapping time (*TT*)

q (L/min)	*Nozzle*	*RR*	*L*	*TT*
0.0260	Left	0.14	9.73	11.09
0.0260	Right	0.12	5.37	7.26
0.0657	Left	0.18	8.29	7.73
0.0657	Right	0.12	4.88	6.43

The obtained values of *RR* and *L* coefficients indicate that pressure fluctuations in the left nozzle are more predictable in comparison with pressure fluctuations in the right nozzle. It is observed for both analysed air volume flow rates. The values of *TT* coefficient point that the dominant frequency of the attractors' trajectory in four-dimensional space is lower in the left nozzle than in the right nozzle. The mentioned differences are greater for lower air volume flow rate. The results of analysis confirms that the frequencies of bubble departures from both nozzles become similar when the air volume flow rate is increased.

4. CONCLUSIONS

In this article, the synchronisation of bubble departures from twin nozzles in engine oils was analysed. In the experiment, the alternative and simultaneous bubble departures were observed.

It has been shown that for the alternative bubble departures, the correlation of air pressure fluctuations in the neighbouring nozzle increases continuously. Finally, it leads to the disappearance of alternative bubble departures. The mentioned process is repeated in a cyclic way.

Non-linear analysis of bubble departure synchronisations proves that the way of bubble departures from two neighbouring nozzles does not depend simply on the character of pressure fluctuations in the nozzle air supply systems. Chaotic changes of the air pressure oscillations do not always determine the chaotic character of bubble departures. Such situations are observed for alternative bubble departures in engine oil. The obtained results confirm the conclusions presented in the article by Vazquez et al. (2010).

REFERENCES

1. **Dzienis P., Mosdorf R.** (2014), Stability of periodic bubble departures at a low frequency, *Chemical Engineering Science,*109, 171-182.
2. **Femat R., Ramirez J.A., Soria A.** (1998), Chaotic flow structure in a vertical bubble column, *Physics Letters A*,248 (1), 67–79.
3. **Grassberger P., and Procaccia I.** (1983), Measuring the strangeness of strange attractors, *Physica - D*,9, 189–208.
4. **Kazakis N.A., Mouza A.A., Paras S.V.** (2008), Coalescence during bubble formation at two neighbouring pores: an experimental study in microscopic scale, *Chemical Engineering Science,*63, 5160–5178
5. **Lavensona D.M., Kelkara A.V., Daniel A. B., Mohammad S.A., Koubab G., Aicheleb C.P.** (2016), Gas evolution rates – A critical uncertainty in challenged gas-liquid separations, *Journal of Petroleum Science and Engineering*, 147, 816-828
6. **Legendre D., Magnaudet J., Mougin G.** (2003), Hydrodynamic interactions between two spherical bubbles rising side by side in a viscous liquid,*Journal of Fluid Mechanics,*497, 133–166.
7. **Marwan N.**(2019), Cross Recurrence Plot Toolbox for Matlab, Ver. 5.15, Release 28.10, http://tocsy.pik-potsdam.de.
8. **Marwan N., Romano M. C., Thiel M., Kurths J.** (2007),Recurrence Plots for the Analysis of Complex Systems,*Physics Reports*, 438, 237 – 329.
9. **Mosdorf R., Dzienis P., Litak G.** (2017), The loss of synchronization between air pressure fluctuations and liquid flow inside the nozzle during the chaotic bubble departures, *Meccanica*, 52, 2641–2654
10. **Mosdorf R., Wyszkowski T.** (2011), Experimental investigations of deterministic chaos appearance in bubbling flow, *International Journal of Heat and Mass Transfer,* 54, 5060–5069.
11. **Mosdorf R., Wyszkowski T.** (2013), Self-organising structure of bubbles departures, *International Journal of Heat and Mass Transfer*, 61, 277–286.
12. **Sanada T., Sato A., Shirota M.T., Watanabe M.** (2009), Motion and coalescence of a pair of bubbles rising side by side, *Chemical Engineering Science*, 64, 2659-2671.
13. **Schuster H.G.** (1993), *Deterministic Chaos. An Introduction*, PWN, Warszawa (in Polish).
14. **Snabre P., Magnifotcham F.** (1997), Formation and rise of a bubble stream in viscous liquid,*European Physical Journal B*, 4, 369-377.
15. **Torrence C., Compo G. P.** (1998), A practical guide to wavelet analysis, *Bulletin of the American Meteorological Society*,79, 61-78.
16. **Vazquez A., Leifer I., Sanchez R.M.** (2010), Consideration of the dynamic forces during bubble growth in a capillary tube, *Chemical Engineering Science*, 65, 4046–4054.
17. **Wolf A., Swift J.B., Swinney H.L., Vastano J.A.** (1985), Determining Lyapunov Exponent from a Time series, *Physica-D*, 16, 285–317.

This work has been accomplished under the research project No. UMO-2011/03/N/ST8/04079 financed by the Polish National Science Center.